Molecular Simulation of Reaction Mechanism for Hemicellulose Model Compound during Chlorine Dioxide Bleaching

Shuangquan Yao,[a,b] Cheng Wang,[a,b] Cong Gao,[a,b] Lisheng Shi,[a,b] Shuangxi Nie,[a,b] and Chengrong Qin [a,b,*]

D-xylose, a hemicellulose model compound, was oxidized by chlorine dioxide under simulated bleaching conditions, and the mechanism of this reaction was investigated. The final reaction product, chloroacetic acid, was detected by gas chromatography-mass spectrometer (GC-MS). To study the generating mechanism of chloroacetic acid by D-xylose during chlorine dioxide bleaching, three reaction pathways were designed. The results showed that the biggest heat of reaction, -234.33 kJ/mol, and the minimum reaction activation energy, 44.44 kJ/mol, appeared for one of the candidate pathways (no. 2). That pathway was thermodynamically more favored. Xylitol was generated by D-xylose degradation, and then chloroacetic acid was generated by a series of oxidation, fracture, and substitution reactions on xylitol.

INTRODUCTION

There is considerable interest and public concern regarding the discharge of pulp bleaching effluents to the environment because they contain high amounts of chlorinated organics that originate from chlorine bleaching (Bouiri and Amrani 2010; Li *et al.* 2016; Saelee *et al.* 2016). One important group of these substances is organic halogens, which are characterized by toxicity and bioaccumulation (Yeh *et al.* 2014; Jaacks and Staimez 2015). The organic halogens can be defined as adsorbable organic halogens (AOX) (Nie *et al.* 2014, 2015; Yao *et al.* 2017). The formation of AOX is an estimate of the soluble and organically bound chlorine in pulp bleaching effluents (Hart and Santos 2013; Fang *et al.* 2016). Pulping processes utilize large amounts of water, and chlorine is still in use in some of the paper pulp producing plants due to the superior quality of the paper produced and the cost-effectiveness of chlorine bleaching. For these reasons, AOX reduction technology has become an advanced research topic (Singh *et al.* 2008; Bouiri and Amrani 2010).

To meet increasingly stringent discharge limits, the amount of AOX discharged from pulp mills can be reduced in two ways: optimization of the mill process and adoption of technologically advanced treatment systems. Optimization of mill processes (Benattar *et al.* 2007) includes lowering the pulp concentration, extending the cooking time, oxygen delignification, increasing chlorine dioxide substitution (Baycan *et al.* 2007), changing the pH in the D_0 stage (first stage of chlorine dioxide bleaching) (the initial pH 2 to 4, and the final pH 8 to 9) (Hart and Connell 2008), and reducing the chlorine dosage during bleaching

as well as subsequent AOX discharges from the bleach plant. External treatments, such as biological treatments, reduce AOX discharge from the mill to the receiving water. Xylanase (Dai *et al.* 2016) and laccase (Pei *et al.* 2016; Nie *et al.* 2018) were evaluated in elemental chlorine free (ECF) bleaching of eucalyptus kraft pulp, and a 34% reduction of AOX in the effluents was observed (Sharma *et al.* 2014). Xylanase pre-treatment can remove HexA and expose more lignin, decreasing the chlorine dioxide demand, thus reducing the formation of AOX (Nie *et al.* 2015). An external chemical treatment has been developed that significantly reduces AOX in bleach plant effluent prior to biological treatment. The inclusion of additives, such as dimethyl sulfoxide (DMSO) (Lachenal *et al.* 2000), hydrogen peroxide (Baycan *et al.* 2007), or amino sulfonic acid, among others, can be considered. For the portion of the lignin that was removed, alkali extraction is an effective method to reduce AOX formation.

The authors also found that hemicellulose affects AOX formation. A pH pre-corrected hot water pretreatment was developed (Yao *et al.* 2015, 2017). The influence of lignin on AOX formation was eliminated by controlling the hot water extraction time, and AOX formation decreased 33% under optimal hot water extraction conditions. In this paper, D-xylose was used as the hemicellulose model compound, and it reacted with chlorine dioxide under simulated bleaching conditions. Then, GC-MS was used to determine the reaction products. The effects of pH, temperature, chlorine dioxide dosage, and D-xylose dosage on AOX formation were investigated. The reaction pathway is calculated by using the molecular simulation technique. The aim of the present work was to appraise the reaction mechanism of the reaction of hemicellulose with chlorine dioxide. This work will provide a theoretical basis for reducing AOX formation based on the perspective of hemicellulose.

EXPERIMENTAL

Materials

D-xylose from corn cob was purchased from Aladdin Reagent Co. LTD (Shanghai, China). Active carbon adsorption columns were purchased from Analytik-Jena Instrument Company (Jena, Germany). Other chemicals were purchased from Aladdin Reagent Co. LTD (Shanghai, China), such as sulfuric acid and sodium hydroxide. All assay reagents were obtained from Sigma-Aldrich Co. (St. Louis, MO, USA), such as chloroacetic acid and furfural. All of the chemicals used were of analytical grade.

Methods
Reaction environment

A Multi X2500 AOX analyzer (Analytik Jena AG, Jena, Germany) was employed to identify AOX in the bleaching effluent (Yao *et al.* 2017) and was applied for kinetics runs. Solutions of D-xylose were prepared and added to a three-neck flask. A sulfuric acid solution and sodium hydroxide were used to adjust the pH of the solution. The reactions were initiated by mixing D-xylose and chlorine dioxide solutions directly in a three-neck flask. All of the reactions were conducted at room temperature (25 °C).

Chemical composition analysis

The chemical composition of the reaction products and content of D-xylose in the reaction solution were quantified by GC-MS (Agilent 6890-5973, Palo Alto, USA) (Kukkola *et al.* 2006; Singh *et al.* 2008). The basic method and process were previously described in a study by Yao *et al.* (2016).

The AOX was formed by the reaction between D-xylose and chlorine dioxide; AOX includes more than 300 different organochlorines (Krzmarzick and Novak 2014). To further understand the reaction mechanism of D-xylose and chlorine dioxide, the specific reaction products need to be analyzed.

Reaction transient analysis

The structure model was constructed by molecular simulation techniques using the visualizer module of Materials Studio (Neotrident Technology Limited, 7.0, Beijing, China). The density functional theory (DFT) calculations were performed using the DMOL3 program (Idupulapati and Mainardi 2008; Vogt *et al.* 2008; Wu *et al.* 2014). To determine the activation energy for a specific reaction pathway, a transition state was identified by the complete linear synchronous transit (LST) and the quadratic synchronous transit (QST) methods. The double numerical plus polarization function (DNP) and the generalized gradient approximation (GGA) functional were used for all geometry optimizations.

RESULTS AND DISCUSSION

Reaction Condition Analysis
Effect of pH on AOX formation

To elucidate the mechanisms of AOX formation, tests were performed with the reaction solution by modifying the pH with sulfuric acid and sodium hydroxide. Research shows that the bleaching solution pH affects the pulp brightness and yield during chlorine dioxide bleaching (Svenson *et al.* 2002, 2006). The best pH value of chlorine dioxide bleaching is 3 to 4 (Francis *et al.* 1997; Catalkaya and Kargi 2007). However, there are few reports describing how the joint action of pH and chlorine ions affect AOX formation in advanced oxidation technologies.
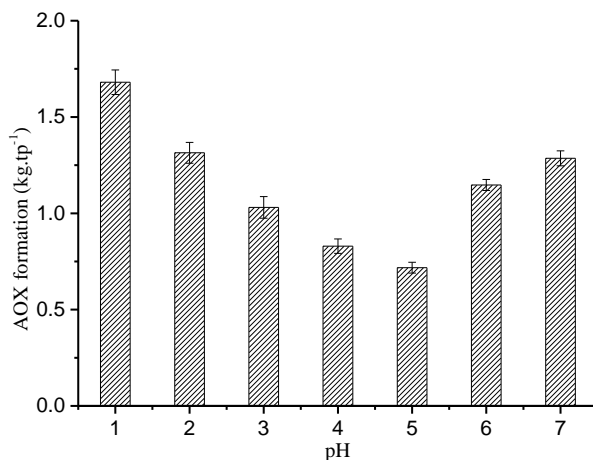

Fig. 1. pH value on influence of AOX formation

The formation of AOX was evaluated during the reaction between chloride ions and D-xylose under different pH (1 to 7) in the bleaching effluent (Fig. 1). The reaction conditions were as follows: 10% (W/W) D-xylose dosage, 2.0% (W/W) chlorine dioxide dosage, temperature 60 °C, and a time of 60 min. The AOX formation decreased as the pH increased from 3 to 4; this result was similar to that reported by Yuan *et al.* (2012). The results shown in Fig. 1 indicated that with sulfuric acid, AOX formation started at a pH of approximately 3 and decreased 19.5% at pH 4, but it decreased 13.5% at pH 5 compared with pH 4. The above phenomenon can be attributed to changes of D-xylose degradation under different pH conditions (Kumar *et al.* 2009; Talebnia *et al.* 2010; Mäki-Arvela *et al.* 2011). This can be attributed to the highest degradation of D-xylose in weak acidic conditions. Large amounts of alcohols, ester, ether, and heterocyclic were generated by the rapid degradation of D-xylose, and the chloride ions had no opportunity to react with D-xylose molecules. The AOX formation increased with pH as the pH increased above pH 5, which indicated that with sodium hydroxide, the formation of AOX started at a pH of approximately 5 and increased to approximately 79.1% at pH 7. The lowest degradation of D-xylose was observed at pH 7, so it was generated by most of xylose molecules that directly reacted with chloride ions in solution. Meanwhile, transformation of hydroxyl radicals by the dissociation of the $ClOH^{-1}$ radical to the hydroxyl radical and chloride ions was favored at high pH (Elmorsi *et al.* 2010; Gao *et al.* 2011). In general, the influence of pH on AOX formation depends on the nature of the reaction substrate.

Effect of ClO_2 on AOX formation

In this experiment, the dosages of ClO_2 changed between 1.0% and 10%. The change in AOX formation with ClO_2 dosage is shown in Fig. 2.
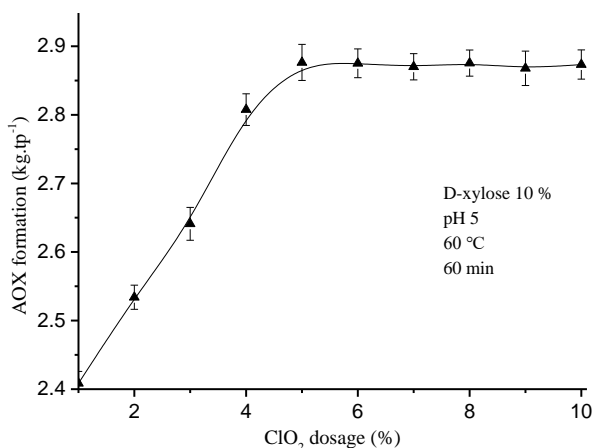

Fig. 2. ClO_2 dosage on influence of AOX formation

The change in AOX formation was divided into two stages. AOX formation increased linearly in the initial reaction within 5.0% ClO_2 dosage. It trended towards saturation as the reaction progressed, and basically remained unchanged after 5.0% ClO_2 dosage. The dosage of ClO_2 was 1.0%, 2.0%, 3.0%, 4.0%, and 5.0%, and they corresponded to the following equilibrium contents of AOX: 2.41 kg.tp^{-1}, 2.53 kg.tp^{-1}, 2.64 kg.tp^{-1}, 2.81 kg.tp^{-1}, and 2.88 kg.tp^{-1}, respectively. Although the equilibrium contents increased as the ClO_2 dosage increased, the rate of growth was relatively stable and did not change with increases in ClO_2 dosage. The growth rate was 5.0%, whether the ClO_2 dosage

bioresources.com

multiplied or not. This could be due to the characteristics of the reaction product, chloroacetic acid, because one of the components in the medium to produce AOX was acetic acid. In fact, acetic acid was generated by D-xylose degradation when D-xylose was added to the reaction solution under acidic conditions, and a substitution reaction of chloride ion ensued. The production rate of AOX was mainly affected by the supply of acetic acid. The promotion of AOX formation was limited even when the concentration of chloride ions in the solution dramatically increased.

Effect of D-xylose on AOX formation

Excessive acetic acid was provided by a 10% D-xylose dosage. To study the effect of D-xylose on AOX formation, the amount of D-xylose added to the reaction was varied under constant reaction conditions. The results are shown in Fig. 3.
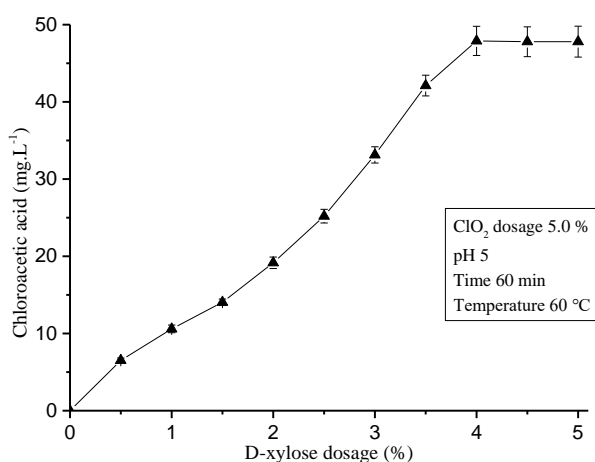

Fig. 3. D-xylose dosage on influence of AOX formation

The change in AOX formation was divided into two stages. AOX formation linearly increased in the initial reaction within 4.0% D-xylose dosage. It basically remained unchanged after 4.0% D-xylose dosage. The equilibrium concentration of AOX was 0.88 kg.tp^{-1} when the D-xylose dosage was 2.0%, and it increased with increasing D-xylose dosage. The rate of change in the AOX formation was similar when D-xylose 2.5% and 3.0% were used in the reaction, but declined when the D-xylose dosage was more than 3.0%, with the highest equilibrium concentration of AOX observed when the D-xylose dosage was 4.0%. Therefore, the saturated dosage of D-xylose was 4.0%.

Effect of temperature and time on AOX formation

The AOX formation at various temperatures (20 °C, 30 °C, 40 °C, 50 °C, and 60 °C) with time is shown in Fig. 4, and was divided into two stages. One stage was a rapid growth stage within 45 min, and the other was the saturation concentration stage after 45 min. The equilibrium concentration of AOX was 1.35 kg.tp^{-1} at 20 °C. It increased as the temperature increased, and was 1.46 kg.tp^{-1}, 1.56 kg.tp^{-1}, 1.66 kg.tp^{-1}, and 1.75 kg.tp^{-1} at 30 °C, 40 °C, 50 °C, and 60 °C, respectively. The growth rate of the equilibrium concentration was stable. There is a linear relationship between the temperature and the formation of AOX.
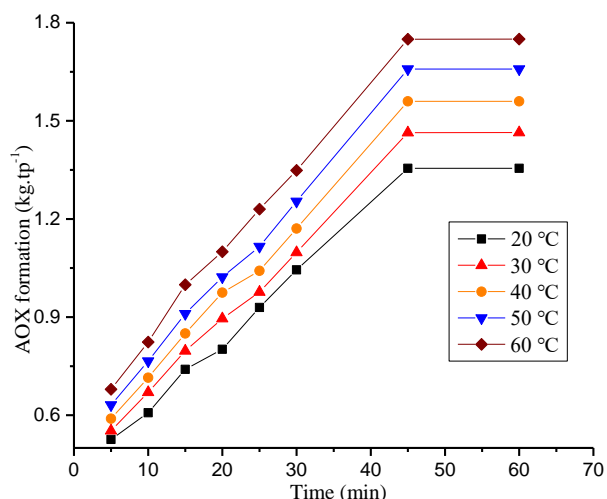
Fig. 4. Temperature and time on influence of AOX formation

Reaction Product Identification

The GC-MS was used to determine the content of various compounds in water samples. The reaction conditions were as follows: 4.5% D-xylose dosage, 4% chlorine dioxide dosage, temperature 60 °C, time 45 min, and pH 5. For the reaction solution samples, some peaks were obtained and are listed in Fig. 5. Many peaks appeared in the chromatograms at various retention times, which indicated that several compounds were contained within the samples. The MS spectrum for each peak was analyzed.
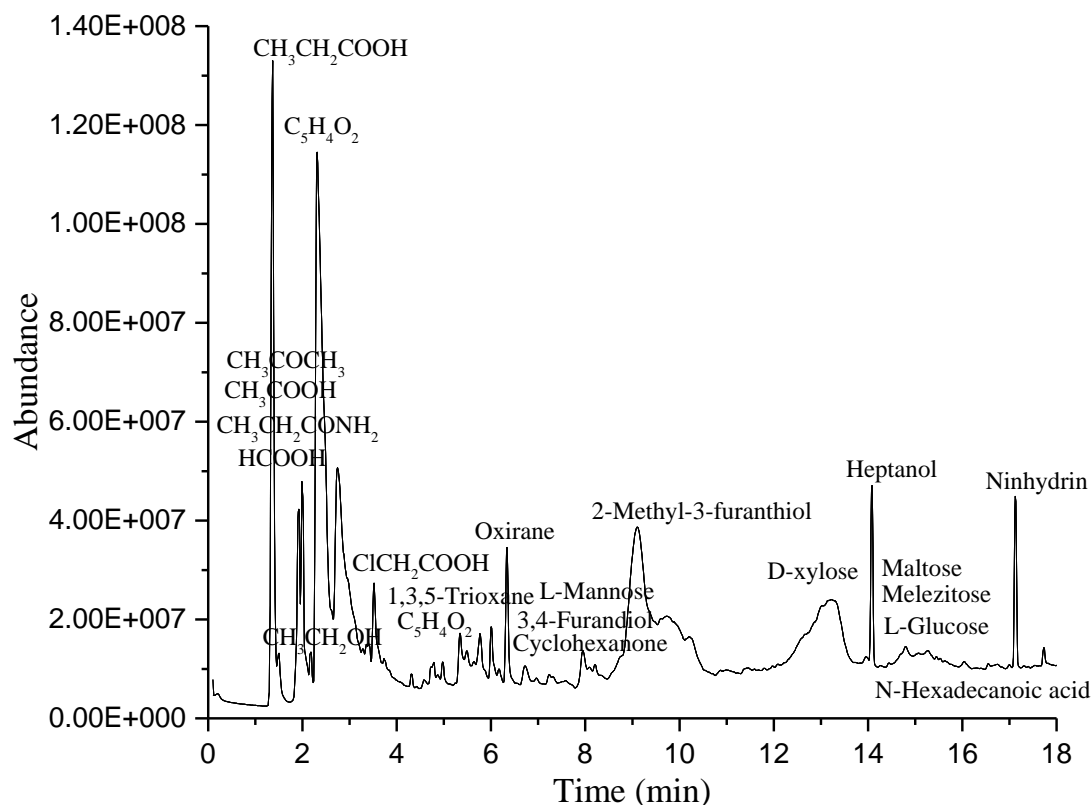

Fig. 5. TIC of the reaction solution

bioresources.com

The only chloride in the water samples after the reaction between D-xylose and chlorine dioxide was chloroacetic acid (3.419 min). The chemical composition of chlorine dioxide bleaching wastewater was detected by GC-MS, and chloroacetic acid was detected, which indicated that the main reaction product was chloroacetic acid. The GC-MS analysis of the samples showed that they contained organic acids and alkalis, such as propanoic acid (1.358 min and 2.007 min), formic acid (1.920 min), acetic acid (2.086 min, 3.419 min, 9.772 min, 9.877 min, and 10.216 min), ethanol (2.307 min), erythritol (2.307 min), and so on. These organic acids and alkalis were produced by D-xylose hydrolysis (Kumar *et al.* 2009).

Many other esters, ethers, and heterocyclic compounds were detected, such as ethyl ether (1.358 min), ethyl acetate (1.491 min), 2-furanone (2.007 min), 2-propanone (2.178 min), furfural (2.626 min, 2.738 min, 2.916 min, 3.284 min, 3.366 min, and so on), glyceraldehyde (4.423 min, 4.510 min, 4.870 min, and 5.153 min), 1,3,5-trioxane (5.488 min and 5.642 min), and so on. These esters, ethers, and heterocyclic compounds were formed by the condensation reactions between the organic acids and alkalis (Sonawane *et al.* 2016). In addition to the above observations, it can be observed that they contain monosaccharides, such as D-arabinose (7.414 min), L-mannose (7.522 min), L-glucose (12.677 min), and xylose (12.740 min). Monosaccharides were formed by the hydrolysis of impurities in the D-xylose samples.

The Molecular Orbital of D-xylose Analysis

The lowest unoccupied molecular orbital (LUMO) and highest occupied molecular orbital (HOMO) of the D-xylose molecule model were calculated and analyzed (Al-Wabli *et al.* 2016; Sworakowski *et al.* 2016).

The HOMO was mainly distributed on the oxygen atoms of the adjacent hydroxyl group. The energy of the HOMO was -0.211eV. The LUMO mainly distributed on five carbons and one oxygen atom that make a ring structure and its energy was -0.040 eV. Therefore, the two adjacent hydroxyl groups of D-xylose (Fig. 6) were vulnerable to the electrophilic reagent attack, and then the dehydration-condensation reaction occurred to form C=C bonds. The C-OH bond was weakened because the electrons on the HOMO were transferred to the neighboring C atoms in the LUMO. Thus, D-xylose had comparatively higher activity.
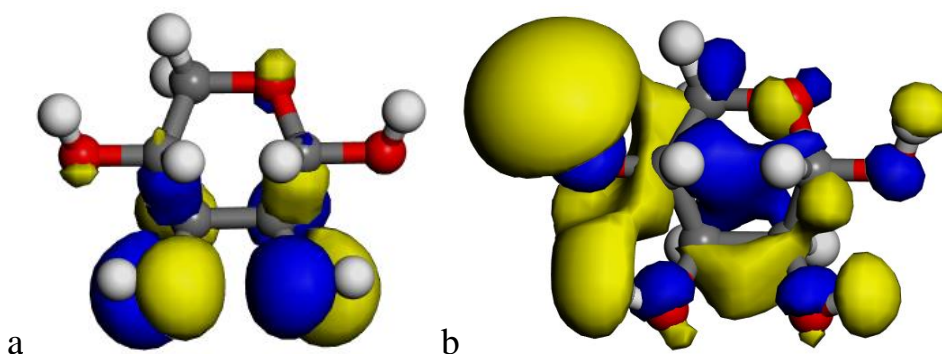

a   b

Fig. 6. The HOMO (a) and LUMO (b) of D-xylose

Proposed Reaction Mechanism

The chemical properties of D-xylose are similar to those of glucose. D-xylose can be reduced to corresponding alcohols including xylitol, which is the most important reduction product (Tani *et al.* 2016; Díaz-Fernández *et al.* 2017; Paidimuddala *et al.* 2017; Sampaio *et al.* 2017; Tani *et al.* 2017). It also can be oxidized to 3-hydroxy-glutarate (Latini *et al.* 2005; Taherdazeh and Karimi 2007; Esteves *et al.* 2008; Cho *et al.* 2011). Therefore, xylitol and 3-hydroxyglutaric acid are intermediate products during the simulated chlorine bleaching process, which has been demonstrated by various experimental analyses in the authors' previous studies (Yao *et al.* 2015, 2017).

There is also the possibility that the chloroacetic acid was produced by oxidation of xylitol or 3-hydroxyglutaric acid. The structure of D-xylose is relatively unstable because it has four neighboring hydroxyl groups. The intermediate product S1 is easily produced in an acidic environment, while S2 is generated by a series of addition and substitution reactions on S1. After that, the chloroacetic acid is produced by an oxidation reaction on S2. Therefore, three reaction pathways of the formation of chloroacetic acid during the reaction between D-xylose and chlorine dioxide were proposed (Fig. 7).
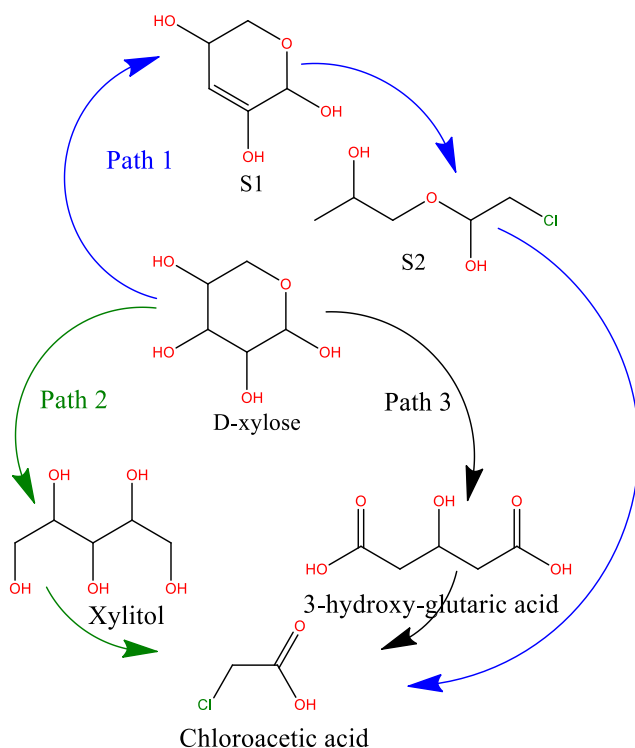

Fig. 7. Suggested reaction pathways

Reaction Pathway Analysis

Density functional theory (DFT) was used to propose a mechanism for this reaction. Three main steps were monitored for pathway 1 during the whole reaction. The model of the intermediates in reaction pathway 1 (Fig. 8) was established by the visualizer module of Materials Studio. All atoms were matching after the structure of the reactants and products was geometrically optimized. The reaction transition state was searched by LST/QST, while the activation energy and the heat of reaction were also obtained.
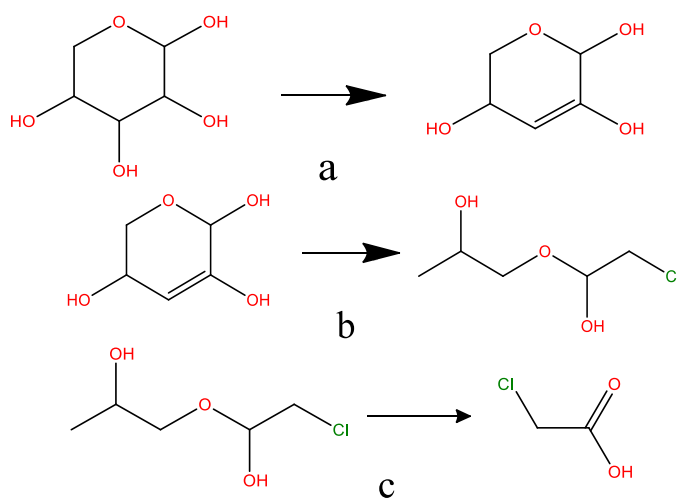
bioresources.com

Fig. 8. Reaction equations of pathway 1

Table 1 shows that the heat of reaction for reaction (1a) was 40.66 kJ/mol. It also shows that the formation of the S1 that has a C=C bond was produced by the dewatering of the hydroxyl group on C2 and C3 of D-xylose, which is an endothermic reaction. The activation energy of reaction (1a) was 57.67 kJ/mol, which indicated that this reaction was more practical. The heats of reaction for reactions (1b) and 1(c) were -192.68 kJ/mol and -39.05 kJ/mol, respectively. The values indicated that the formation of the intermediate product S2 and chloroacetic acid was an exothermic reaction. Among these three reactions, the activation energy of reaction (1b) was 12.44 kJ/mol, which showed that reaction (1b) was the easiest and also the fastest one according to the Arrhenius equation (Gaona-Colmán *et al.* 2017). The total activation energy and the total reaction heat of the reaction of pathway 1 were 96.01 kJ/mol and -131.72 kJ/mol, respectively.

Table 1. Activation Energy (ΔE) and Heat of Reaction (ΔH) of Reactions

Pathway	Reaction	ΔE (kJ/mol)	ΔH (kJ/mol)
1	a	57.67	40.66
	b	12.44	-192.68
	c	25.90	-39.05
2	a	19.33	-97.26
	b	8.48	-134.49
	c	16.63	-2.58
3	a	22.97	-34.92
	b	36.50	43.64
	c	14.13	-73.89

Reaction pathway 2 involved a three-step response (Fig. 9). The first step was reducing D-xylose to xylitol. The second step was the production of hydroxyacetic acid by the oxidation of xylitol. The chloroacetic acid was produced as hydroxyacetic acid, which has strong activity to easily react with chlorine ions in solution. Figure 9 shows the reaction equations of pathway 2. The activation energy and heat of reaction for each step during the reactions of pathway 2 were obtained.
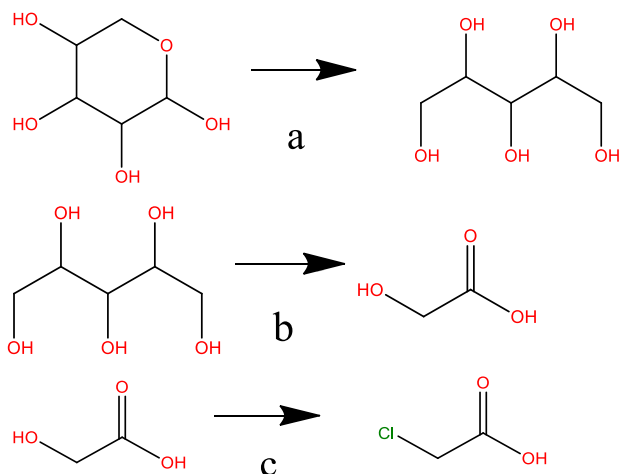
Fig. 9. Reaction equations of pathway 2

From Table 1, the reaction heat of reaction (2a) was -97.26 kJ/mol, which showed that the formation of xylitol that was produced by the degradation of D-xylose was an exothermic reaction. The activation energy of reaction (2a) was 19.33 kJ/mol, which indicated that this reaction was practical. The heat of reaction for reactions (2b) and (2c) was -134.49 kJ/mol and -2.58 kJ/mol, respectively, which showed that the formation of hydroxyacetic acid and chloroacetic acid was an exothermic reaction. The activation energy of these two reactions was 8.48 kJ/mol and 16.63 kJ/mol, respectively, which indicated that reactions (2b) and (2c) were even more practical than reaction (a). Therefore, in reaction pathway 2, the activation energy of reaction (2c) was the lowest and the reaction rate of reaction (2c) was the fastest among these three reactions. The total activation energy and the total reaction heat of reaction pathway 2 were 44.44 kJ/mol and -234.33 kJ/mol, respectively. In previous studies, Converti and Domínguez (Converti and Domínguez 2001; Converti *et al.* 2003) found that the reaction heat of the formation of xylitol produced by the degradation of D-xylose was between -162.0 kJ/mol and -296.1 kJ/mol, while Liu *et al.* (2012) figured out that the apparent activation energy of the reaction was 46.33 kJ/mol. These results indicated that the calculated results were valid.
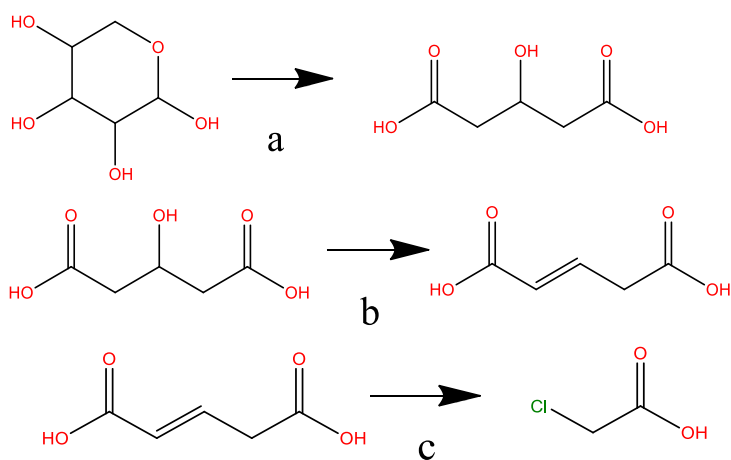

Fig. 10. Reaction equations of pathway 3

Reaction pathway 3 was a three-step response as well (Fig. 10). The first step was that D-xylose was oxidized to 3-hydroxy-glutarate. The second step was production of pentenedioic acid by the intramolecular dehydration of 3-hydroxy-glutarate. Because the structure of pentenedioic acid is unstable, the C=C bond was easily broken after oxidation. The chloroacetic acid was produced as the chlorine substitution that occurred after the break of pentenedioic acid was due to oxidation. The results are shown in Fig. 10. The activation energy and heat of reaction for each step of reaction pathway 3 was obtained.

From Table 1, the heat of reaction for reactions (3a) and (3c) was -34.92 kJ/mol and -73.89 kJ/mol, respectively. Therefore, it was proposed that the formation of 3-hydroxy-glutarate and chloroacetic acid was an exothermic reaction. However, the heat of reaction for reaction (3b) was 43.64 kJ/mol, which showed that the formation of pentenedioic acid was an endothermic reaction. The activation energy of reactions (3a) and (3c) was 22.97 kJ/mol and 14.13 kJ/mol, respectively. The activation energy of reaction (3b) was 36.50 kJ/mol, and it was an endothermic reaction. Therefore, reaction (3b) was more difficult to occur than the other two reactions. Compared with reaction (3a) and (3b), reaction (3c) had the lowest activation energy and the fastest reaction rate in reaction pathway 3. The total activation energy and the total heat of reaction for reaction pathway 3 were 73.60 kJ/mol and -65.17 kJ/mol, respectively.

In conclusion, reaction pathway 2 had the lowest activation energy at 44.44 kJ/mol. Therefore, it seemed that pathway 2 was more favorable as the reaction in which xylitol was generated by D-xylose degradation, and then chloroacetic acid was generated by a series of oxidation, fracture, and substitution reactions on xylitol.

CONCLUSIONS

1. The final product of the reaction between hemicellulose and chlorine dioxide during the bleaching process was chloroacetic acid. Among three suggested reaction pathways, reaction pathway 2 was optimal because it had the highest heat of reaction and the lowest activation energy for the reaction.

2. Xylitol was generated by D-xylose degradation, and then chloroacetic acid was generated by a series of oxidation, fracture, and substitution reactions on xylitol. The results provide a new way to resolve the biggest environmental pollution problem during the ECF bleaching process.

ACKNOWLEDGMENTS

bioresources.com

REFERENCES CITED

Al-Wabli, R. I., Resmi, K. S., Mary, Y. S., Panicker, C. Y., Attia, M. A., El-Emam, A. A., and Alsenoy, C. V. (2016). "Vibrational spectroscopic studies, Fukui functions, HOMO-LUMO, NLO, NBO analysis and molecular docking study of (E)-1-(1,3-benzodioxol-5-yl)-4,4-dimethylpent-1-en-3-one, a potential precursor to bioactive agents," *J. Mol. Struct.* 1123, 375-383. DOI: 10.1016/j.molstruc.2016.07.044

Baycan, N., Thomanetz, E., and Sengül, F. (2007). "Influence of chloride concentration on the formation of AOX in UV oxidative system," *J. Hazard. Mater.* 143(1-2), 171-176. DOI: 10.1016/j.jhazmat.2006.09.010

Benattar, N., Calais, C., Hamzeh, Y., and Mortha, G. (2007). "Modified ECF bleach-ing sequences optimizing the use of chlorine dioxide," *Appita J.* 60, 150-154.

Bouiri, B., and Amrani, M. (2010). "Elemental chlorine-free bleaching halfa pulp," *J. Ind. Eng. Chem.* 16(4), 587-592. DOI: 10.1016/j.jiec.2010.03.015

Catalkaya, E. C., and Kargi, F. (2007). "Color, TOC and AOX removals from pulp mill effluent by advanced oxidation processes: A comparative study," *J. Hazard. Mater.* 139(2), 244-253. DOI: 10.1016/j.jhazmat.2006.06.023

Cho, D. H., Kim, Y. H., Kim, B.-R., Park, J.-M., Sung, Y.-J., and Shin, S.-J. (2011). "Kinetic study of xylan hydrolysis and decomposition in concentrated sulfuric acid hydrolysis process by 1H-NMR spectroscopy," *Palpu Chongi Gisul/J. Korea TAPPI* 43(3), 52-58.

Converti, A., and Domínguez, J. M. (2001). "Influence of temperature and pH on xylitol production from xylose by *Debaryomyces hansenii*," *Biotechnol. Bioeng.* 75(1), 39-45. DOI: 10.1002/bit.1162

Converti, A., Torre, P., de Luca, E., Perego, P., Del Borghi, M., and da Silva, S. S. (2003). "Continuous xylitol production from synthetic xylose solutions by *Candida guilliermondii*: Influence of pH and temperature," *Eng. Life Sci.* 3(4), 193-198. DOI: 10.1002/elsc.200390027

Dai, Y., Song, X., Gao, C., He, S., Nie, S., and Qin, C. (2016). "Xylanase-aided chlorine dioxide bleaching of bagasse pulp to reduce AOX formation," *BioResources* 11(2), 3204-3214. DOI: 10.15376/biores.11.2.3204-3214

Díaz-Fernández, D., Lozano-Martínez, P., Buey, R. M., Revuelta, J. L., and Jiménez, A. (2017). "Utilization of xylose by engineered strains of *Ashbya gossypii* for the production of microbial oils," *Biotechnol. Biofuels* 10(3), 1-12. DOI: 10.1186/s13068-016-0685-9

Elmorsi, T. M., Riyad, Y. M., Mohamed, Z. H., and Abd El Bary, H. (2010). "Decolorization of Mordant red 73 azo dye in water using H_2O_2/UV and photo-Fenton treatment," *J. Hazard. Mater.* 174(1-3), 352-358. DOI: 10.1016/j.jhazmat.2009.09.057

Esteves, B., Graça, J., and Pereira, H. (2008). "Extractive composition and summative chemical analysis of thermally treated eucalypt wood," *Holzforschung* 62(3), 344-351. DOI: 10.1515/HF.2008.057

Fang, C., Xiao, D., Liu, W., Lou, X., Zhou, J., Wang, Z., and Liu, J. (2016). "Enhanced AOX accumulation and aquatic toxicity during 2,4,6-trichlorophenol degradation in a Co(II)/peroxymonosulfate/Cl⁻ system," *Chemosphere* 144, 2415-2420. DOI: 10.1016/j.chemosphere.2015.11.030

Francis, D., Turner, P., and Wearing, J. (1997). "AOX reduction of kraft bleach plant effluent by chemical pretreatment—Pilot-scale trials," *Water Res.* 31(10), 2397-2404. DOI: 10.1016/S0043-1354(97)00058-4

Gao, B., Yap, P. S., Lim, T. M., and Lim, T.-T. (2011). "Adsorption-photocatalytic degradation of Acid Red 88 by supported TiO_2: Effect of activated carbon support and aqueous anions," *Chem. Eng. J.* 171(3), 1098-1107. DOI: 10.1016/j.cej.2011.05.006

Gaona-Colmán, E., Blanco, M. B., Barnes, I., Wiesen, P., and Teruel, M. A. (2017). "OH- and O_3-initiated atmospheric degradation of camphene: Temperature dependent rate coefficients, product yields and mechanisms," *RSC Adv.* 7(5), 2733-2744. DOI: 10.1039/c6ra26656h

Hart, P. W., and Connell, D. (2008). "Improving chlorine dioxide bleaching efficiency by selecting the optimum pH targets," *TAPPI J.* 7, 3-11.

Hart, P. W., and Santos, R. B. (2013). "Kraft ECF pulp bleaching: A review of the development and use of techno-economic models to optimize cost, performance, and justify capital expenditures," *TAPPI J.* 12, 19-29.

Idupulapati, N., and Mainardi, D. (2008). "A DMol^3 study of the methanol addition–elimination oxidation mechanism by methanol dehydrogenase enzyme," *Mol. Simulat.* 34(10-15), 1057-1064. DOI: 10.1080/08927020802235656

Jaacks, L. M., and Staimez, L. R. (2015). "Association of persistent organic pollutants and non-persistent pesticides with diabetes and diabetes-related health outcomes in Asia: A systematic review," *Environ. Int.* 76, 57-70. DOI: 10.1016/j.envint.2014.12.001

Krzmarzick, M. J., and Novak, P. J. (2014). "Removal of chlorinated organic compounds during wastewater treatment: Achievements and limits," *Appl. Microbiol. Biot.* 98(14), 6233-6242. DOI: 10.1007/s00253-014-5800-x

Kukkola, J., Knuutinen, J., Paasivirta, J., Herve, S., Pessala, P., and Schultz, E. (2006). "Characterization of high molecular mass material in ECF and TCF bleaching liquors by Py-GC/MS with and without TMAH methylation," *J. Anal. Appl. Pyrol.* 76(1-2), 214-221. DOI: 10.1016/j.jaap.2005.11.006

Kumar, P., Barrett, D. M., Delwiche, M. J., and Stroeve, P. (2009). "Methods for pretreatment of lignocellulosic biomass for efficient hydrolysis and biofuel production," *Ind. Eng. Chem. Res.* 48(8), 3713-3729. DOI: 10.1021/ie801542g

Lachenal, D., Joncourt, M. J., Froment, P., and Chirat, C. (2000). "Reduction of AOX formation during chlorine dioxide bleaching," *TAPPI J.* 83, 144-148.

Latini, A., Rodriguez, M., Rosa, R. B., Scussiato, K., Leipnitz, G., Reis de Assis, D., da Costa Ferreira, G., Funchal, C., Jacques-Silva, M. C., Buzin, L., *et al.* (2005). "3-Hydroxyglutaric acid moderately impairs energy metabolism in brain of young rats," *Neuroscience* 135(1), 111-120. DOI: 10.1016/j.neuroscience.2005.05.013

Li, K., Zheng, H., Zhang, H., Zhang, W., Li, K., and Xu, J. (2016). "A novel approach to the fabrication of bleached shellac by totally chlorine-free (TCF) bleaching method," *RSC Adv.* 6, 55618-55625. DOI: 10.1039/C6RA09132F

Liu, W., Yang, T.-Z., Zhou, Q.-H., Zhang, D.-C., and Lei, C.-M. (2012). "Electrodeposition of Sb(III) in alkaline solutions containing xylitol," *Transactions of Nonferrous Metals Society of China* 22(4), 949-957. DOI: 10.1016/S1003-6326(11)61269-7

Mäki-Arvela, P., Salmi, T., Holmbom, B., Willför, S., and Murzin, D. Y. (2011). "Synthesis of sugars by hydrolysis of hemicelluloses-A review," *Chem. Rev.* 111(9),

5638-5666. DOI: 10.1021/cr2000042

Nie, S., Liu, X., Wu, Z., Zhan, L., Yin, G., Yao, S., Song, H., and Wang, S. (2014). "Kinetics study of oxidation of the lignin model compounds by chlorine dioxide," *Chem. Eng. J.* 241, 410-417. DOI: 10.1016/j.cej.2013.10.068

Nie, S., Wang, S., Qin, C., Yao, S., Ebonka, J. F., Song, X., and Li, K. (2015). "Removal of hexenuronic acid by xylanase to reduce adsorbable organic halides formation in chlorine dioxide bleaching of bagasse pulp," *Bioresource Technol.* 196, 413-417. DOI: 10.1016/j.biortech.2015.07.115

Nie, S., Zhang, K., Lin, X., Zhang, C., Yan, D., Liang, H., and Wang S. (2018). "Enzymatic pretreatment for the improvement of dispersion and film properties of cellulose nanofibrils," *Carbohyd. Polym.* 181, 1136-1142, DOI: 10.1016/j.carbpol.2017.11.020

Paidimuddala, B., Rathod, A., and Gummadi, S. N. (2017). "Inhibition of *Debaryomyces nepalensis* xylose reductase by lignocellulose derived by-products," *Biochem. Eng. J.* 121, 73-82. DOI: 10.1016/j.bej.2017.01.019

Pei, Y., Wang, S., Qin, C., Su, J., Nie, S., and Song, X. (2016). "Optimization of laccase-aided chlorine dioxide bleaching of bagasse pulp," *BioResources* 11(1), 696-712. DOI: 10.15376/biores.11.1.696-712

Saelee, K., Yingkamhaeng, N., Nimchua, T., and Sukyai, P. (2016). "An environmentally friendly xylanase-assisted pretreatment for cellulose nanofibrils isolation from sugarcane bagasse by high-pressure homogenization," *Ind. Crop. Prod.* 82, 149-160. DOI: 10.1016/j.indcrop.2015.11.064

Sampaio, F. C., de Faria, J. T., de Lima Silva, G. D., Gonçalves, R. M., Pitangui, C. G., Casazza, A. A., Al Arni, S., and Converti, A. (2017). "Comparison of response surface methodology and artificial neural network for modeling xylose-to-xylitol bioconversion," *Chem. Eng. Technol.* 40(1), 122-129. DOI: 10.1002/ceat.201600066

Sharma, A., Thakur, V. V., Shrivastava, A., Jain, R. K., Mathur, R. M., Gupta, R., and Kuhad, R. C. (2014). "Xylanase and laccase based enzymatic kraft pulp bleaching reduces adsorbable organic halogen (AOX) in bleach effluents: A pilot scale study," *Bioresource Technol.* 169, 96-102. DOI: 10.1016/j.biortech.2014.06.066

Singh, S., Chandra, R., Patel, D. K., Reddy, M. M. K., and Rai, V. (2008). "Investigation of the biotransformation of pentachlorophenol and pulp paper mill effluent decolorisation by the bacterial strains in a mixed culture," *Bioresource Technol.* 99(13), 5703-5709. DOI: 10.1016/j.biortech.2007.10.022

Sonawane, S. H., Anniyappan, M., Athar, J., Banerjee, S., and Sikder, A. K. (2016). "Synthesis of bis(propargyl) aromatic esters and ethers: A potential replacement for isocyanate based curators," *RSC Adv.* 6(10), 8495-8502. DOI: 10.1039/C5RA25909F

Svenson, D. R., Kadla. J. F., Chang, H.-M., and Jameel, H. (2002). "Effect of pH on the inorganic species involved in a chlorine dioxide reaction system," *Ind. Eng. Chem. Res*. 41(24), 5927-5933. DOI: 10.1021/ie020191+

Svenson, D. R., Jameel, H., Chang, H. M., and Kadla. J. F.(2006). "Inorganic reactions in chlorine dioxide bleaching of softwood kraft pulp," *J. Wood Chem. Technol*. 26(3), 201-213. DOI: 10.1080/02773810601023255

Sworakowski, J., Lipiński, J., and Janus, K. (2016). "On the reliability of determination of energies of HOMO and LUMO levels in organic semiconductors from electrochemical measurements. A simple picture based on the electrostatic model," *Org. Electron.* 33, 300-310. DOI: 10.1016/j.orgel.2016.03.031

Taherdazeh, M. J., and Karimi, K. (2007). "Acid-based hydrolysis processes for ethanol from lignocellulosic materials: A review," *BioResources* 2(3), 472-499. DOI: 10.15376/biores.2.3.472-499

Talebnia, F., Karakashev, D., and Angelidaki, I. (2010). "Production of bioethanol from wheat straw: An overview on pretreatment, hydrolysis and fermentation," *Bioresource Technol.* 101(13), 4744-4753. DOI: 10.1016/j.biortech.2009.11.080

Tani, T., Taguchi, H., and Akamatsu, T. (2017). "Analysis of metabolisms and transports of xylitol using xylose- and xylitol-assimilating *Saccharomyces cerevisiae*," *J. Biosci. Bioeng.* 123(5), 613-620. DOI: 10.1016/j.jbiosc.2016.12.012

Tani, T., Taguchi, H., Fujimori, K. E., Sahara, T., Ohgiya, S., Kamagata, Y., and Akamatsu, T. (2016). "Isolation and characterization of xylitol-assimilating mutants of recombinant *Saccharomyces cerevisiae*," *J. Biosci. Bioeng.* 122(4), 446-455. DOI: 10.1016/j.jbiosc.2016.03.008

Vogt, F. G., Katrincic, L. M., Long, S. T., Mueller, R. L., Carlton, R. A., Sun, Y. T., Johnson, M. N., Copley, R. C. B., and, Light, M. E. (2008). "Enantiotropically-related polymorphs of {4-(4-chloro-3-fluorophenyl)-2-[4-(methyloxy)phenyl]-1,3-thiazol-5-yl} acetic acid: Crystal structures and multinuclear solid-state NMR," *J. Pharm. Sci.* 97(11), 4756-4782. DOI: 10.1002/jps.21336

Wu, Y., Xiao, J., Wu, L., Chen, M., Xi, H., Li, Z., and Wang, H. (2014). "Adsorptive denitrogenation of fuel over metal organic frameworks: Effect of N-types and adsorption mechanisms," *J. Phys. Chem. C* 118(39), 22533-22543. DOI: 10.1021/jp5045817

Yao, S., Gao, C., Zhu, H., Zhang, Y., Wang, S., and Qin, C. (2016). "Effects of additives on absorbable organic halide reduction in elemental chlorine-free bleaching of bagasse kraft pulp," *BioResources* 11(1), 996-1006. DOI: 10.15376/biores.11.1.996-1006

Yao, S., Nie, S., Yuan, Y., Wang, S., and Qin, C. (2015). "Efficient extraction of bagasse hemicelluloses and characterization of solid remainder," *Bioresource Technol.* 185, 21-27. DOI: 10.1016/j.biortech.2015.02.052

Yao, S., Nie, S., Zhu, H., Wang, S., Song, X., and Qin, C. (2017). "Extraction of hemicellulose by hot water to reduce adsorbable organic halogen formation in chlorine dioxide bleaching of bagasse pulp," *Ind. Crop. Prod.* 96, 178-185. DOI: 10.1016/j.indcrop.2016.11.046

Yeh, R. Y. L., Farré, M. J., Stalter, D., Tang, J. Y. M., Molendijk, J., and Esther, B. I. (2014). "Bioanalytical and chemical evaluation of disinfection by-products in swimming pool water," *Water Res.* 59, 172-184. DOI: 10.1016/j.watres.2014.04.002

Yuan, R., Ramjaun, S. N., Wang, Z., and Liu, J. (2012). "Photocatalytic degradation and chlorination of azo dye in saline wastewater: Kinetics and AOX formation," *Chem. Eng. J.* 192, 171-178. DOI: 10.1016/j.cej.2012.03.080